Particle Interactions With Obliquely Propagating Magnetosonic Waves: Energization And/Or Trapping.

Krishna M. Srivastava and Bruce T. Tsurutani

(Jet Propulsion Laboratory, California Institute of Technology, 4800 Oak Grove Drive, Pasadena CA-91 109)

ABSTRACT

Four cases of nonlinear obliquely propagating MS waves are considered using a test particle approach: i) monochromatic waves propagating both sunward and anti-sunward, ii) monochromatic waves propagating unidirectionally towards the Sun, ii) a broad band spectrum, propagating both sunward and anti-sunward, iv) a broad band spectrum, propagating sunward only. As the solar wind decelerates rapidly inside the bow shock due to mass loading, the interplanetary magnetic field increases. Calculations have been performed taking into account of a spatially dependent IMF based on observations. We find significant particle trapping and acceleration for the monochromatic oblique waves. For the "turbulent" case, it is found that for oblique propagation (angle between the interplanetary magnetic field and the propagation vector is larger than 30 degrees), the particles are again highly accelerated but the trapping is very much suppressed due to stochasticity. We compare the relative heating and acceleration for the four cases and discuss the physical mechanisms of trapping and acceleration, Pitch angle scattering and acceleration of particles are found to be much larger in the case of sunward and anti-sunward propagating waves than those for the sunward waves only. This is because of the different stochastic effects associated with the two cases resulting in larger power for sunward and anti-sunward propagating waves than that for the sunward propagating waves only. The electromagnetic trapping of particles in the case of sunward and anti-sunward propagating waves is less than that in the case of sunward propagating waves only. Also the trapping of particles is more in the case of a uniform magnetic field than that in the case of spatially increasing magnetic field resulting in more pitch angle scattering and acceleration.

Subject Headings: Comets, particle scattering, Magnetosonic waves,

INTRODUCTION

The observations made during the encounter with comet Giacobini Zinner show that close to the bow shock the character of MHD turbulence is governed by the magnetosonic waves generated by the pick-up ions via a resonant cyclotron instability (*Tsurutani* et al., 1987). Because the low frequency magnetosonic waves detected at comet Giacobini-Zinner and upstream of Earth's foreshock have similar origin and similar plasma conditions (β of order of unity), their nonlinear development may therefore be analogous. The comet Halley waves have the same origin as the G-Z waves, but the former have lower amplitudes 'and are more turbulent, The IMF is usually at the Parker's spiral angle relative to the solar wind (α = 45° at 1 A.U.), but it ranges from the quasiparallel ($0<\alpha<55°$) to quasiperpendicular regimes ($55°<\alpha<90°$). Cometary waves generally propagate at angles greater than 15° from the IMF, with some at much larger angles (*Tsurutani*, 1991 a, b). The waves at the Earth's foreshock propagate at angles greater than 10° from the IMF. The waves in the solar corona propagate at 10" to 25" to IMF (*Tsurutani*, 1991 a, b). The MS waves at Jupiter have been observed propagating at angles greater than 40" to IMF (*Tsurutani, 1993).*

Coates et al. (1989, 1990) showed that pitch-angle scattering of cometary ions increased with reduced cometocentric distance and was much more efficient than the energy diffusion. Neugebauer et al. (1989, 1990) further concluded that i) the mean width of the proton pitch angle distribution remained relatively low and was nearly independent of cometocentric distance almost right up to the bow shock and ii) the mean width of the water group ion pitch angle distributions increased both with increasing ion density and with increasing α.

The pitch angle scattering (PAS) and acceleration of cometary ions in the mass loaded solar wind by nonlinear monochromatic MS waves propagating unidirectionally towards the sun and also in the presence of "turbulent" spectrum generated by MS waves has been studied using a test particle approach by Srivastava et al., (1992; 1993). Pitch angle scattering, energy diffusion width and distribution functions were obtained. The particle velocity and acceleration were found to increase with increasing wave amplitude, inclination of the wave vector to the background magnetic field and the range of resonant mode numbers. It was shown that nonlinear magnetosonic waves propagating obliquely to the IMF ($\theta_{Bk} > 30^{\circ}$) are very efficient at accelerating the particles because of the high phase velocity ($V_{phase\|} = V_{phase} / \cos\theta_{Bk}$) along the magnetic field. Further, it was found that Landau damping plays an important role in the case of monochromatic MS waves and particles are trapped in a potential well,

Johnstone et al., (1992) have analyzed the spectrum of MHD waves in the solar wind upstream from the bow shock at comet Halley by using data from positive ion analyzers and magnetometers onboard the Giotto spacecraft. The use of Elsasser variables allowed the spectrum of upstream propagating waves to be separated from that of the downstream propagating waves. There was excellent quantative agreement between the observed and calculated spectra in intensity and shape for waves propagating in both directions.

This paper attempts a comparative study of the rate of pitch angle scattering and acceleration of particles induced by interactions via a cyclotron resonance with i) monochromatic waves propagating both sunward and anti-sunward, ii) monochromatic waves propagating sunward unidirectionally, iii) a broad band spectrum, propagating both sunward and anti-sunward, and iv) a broad band spectrum, propagating sunward only, The present study differs from the earlier one (Srivastava et al., 1993) in three respects: i) MS waves propagating both sunward and antisunward are considered, ii) a

spatially dependent IMF based on observations is taken, iii) results of circularly polarized waves are compared with elliptically polarized waves. The paper is organized as follows: in section 2 we discuss the model and the basic ideas. In section 3, we compare numerical results for the four cases for a uniform IMF and the observation' MF. A summary of results is given in section 4.

FORMULATION OF THE PROBLEM

a) The Model:

The geometry of the simulation system is shown in Fig. (l). The background interplanetary magnetic field is represented by

$$B_0 = i\, B_0 \cos\theta_{Bk} + j\, B.\ \sin\theta_{Bk} \qquad (1)$$

where θ_{Bk} is the angle the magnetic field makes with the k-vector and i, j, k are the unit vectors along x, y, z axes with x axis pointing towards the Sun. When the IMF is taken as uniform throughout $B_0 = B_{0\infty}$, the magnetic field components along x and y axes after normalizing by $B_{0\infty}$ are given by $\cos\theta_{Bk}$ and $\sin\theta_{Bk}$. In the realistic case, B_0 *is* not uniform. To take account of the space dependence of the IMF, we take B_{0x} as uniform because divB must vanish, whereas *BOY* is a variable which obeys *BOY(X) U(x)* = $B_{0\infty y}$ U_∞ . *Normalizing* BOY by $B_{0\infty}$ and $U(x)$ by U_∞ , *we* obtain nondimensional equation for B_{0y} as

$$B_{0y}(x)/B_{0\infty} = B^*_{0y}(x) = \sin\theta_{Bk} / U^*(x) \qquad (2)$$

where $\sin\theta_{Bk} = B_{0\infty y} / B_{0\infty}$. $U(x)$, U_∞ , and $B_{0\infty}$ denote, respectively, the solar wind speeds at distances x and infinity from the comet nucleus, and the magnetic field at infinity.

The solar wind speed is a function of cometocentric distance, r. In our simulation model, the distance x along the sun-comet line takes the role of r. The solar wind slows down due to mass loading which first occurs at x=3.4x 10^6km (*Neugebauer* et al., 1990). The solar wind speed remains almost constant prior to the initiation of mass loading. When the cometocentric distance is less than 3.4 Mkm, the solar wind speed decreases moderately at first, but drops rapidly near the bow shock x =1,3 x 106 km. Huddleston et al., (1990) have given a model which gives solar wind speed along any flow line, For our purpose, we assume that the solar wind speed is a simple linear function of the cometocentric distance x along the sun-comet line. According to the observations, the solar wind speed profile can be specified as (Ye and Cravens, 1993):

$$U_{SW}(km/s) = \begin{cases} 365.0 & x(Mkm) > 3.5 \\ 300.0 + (x(Mkm) - 1.4)\ 30.95 & 3.5 > x(Mkm) > 1.4 \\ 280,0 + (x(Mkm) - 1.3)\ 200.0 & 1.4 > x(Mkm) > 1.3 \\ 208.0 + (x(Mkm) - 0.1)\ 60.0 & 1.3 > x(Mkm) > 0.1 \end{cases} \quad (3)$$

The simulation system lies wholly inside the bow shock. For the two comets, viz., G-Z and Halley, the length, L, of the simulation system (the interaction region) considered is:

$1.0 \times 10^5\ km < x < 3.0 \times 10^5\ km$ for G-Z, $L_{G\text{-}Z} = 2 \times 10^5\ km$

$4.0 \times 10^5\ km < x < 12.0 \times 10^5\ km$ for Halley, $L_{Halley} = 8 \times 10^5$ km

b) Wave-Particle Interactions:

We investigate, by using test particle method, the interaction of the cometary pick-up ions with obliquely propagating magnetosonic waves where these waves satisfy the cyclotron resonance condition,

$$\omega - \bar{k} \cdot \bar{v} - \Omega_i = 0 \qquad (4)$$

Here, ω is the frequency of the magnetosonic wave, $\bar{k}$ is the propagation vector, $\bar{v}$ the velocity vector and Ω_i the ion Larmor frequency of water group ion, The MHD dispersion relation of the fast magnetosonic waves is given by

$$\omega^2 = k^2 c_A^2 ((1 + C_1)/2 + C_2)) \qquad (5)$$

where $C_2 = ((1 + C_1)^2/4 - C_1 \cos^2\theta_{Bk}))^{1/2}$

and $C_1 = (c_S / c_A)^2$ and c_S, CA are the sound and Alfven speeds,

It is noted from the observations that steepened MS waves are comprised of circular polarized wave fronts and linearly polarized trailing wave portions. There are also (sometimes) whistler packets leading the *MS* waves. From a spectral analysis under proper conditions it was found that γ varies from -1.6 to -2.5. Thus we have attempted to simulate wave-particle interactions with four "wave types" using test particle approach by following the motion of cometary ions in a given field. Test particle calculations are performed by following the motion of cometary ions in a given field for four cases: i) monochromatic waves propagating both sunward and anti-sunward, ii) monochromatic waves propagating unidirectionally towards the Sun, iii) a broad band spectrum,

propagating both sunward and anti-sunward, iv) a broad band spectrum, propagating sunward only. The power spectrum of both the waves, viz., propagating sunward and anti-sunward is assumed to vary as k^{-2}.

Case i) First we consider the particle interactions with both the elliptically and circularly polarized monochromatic magnetosonic (MS) waves propagating along positive and negative direction to the x-axis (sunward and anti-sunward) obliquely to the background magnetic field Fig. 1. For monochromatic elliptically polarized magnetosonic waves ($EPMSW$) propagating along x, we can write the components of the wave magnetic field in the form

$$B_Y = A_{0y} \cos(kx - \omega t + \Phi_o) \tag{6}$$

$$B_z = A_{0z} \sin(kx - \omega t + \Phi_o) \tag{7}$$

where k, ω, and Φ_0 denote the wave number, the frequency and phase of the wave. A_{0y} and A_{0z} are wave amplitudes in they and z directions. For $A_{0y} = A_{0z}$ we get circularly polarized magnetosonic waves ($CPMSW$).

In the representation shown in Fig. 2, the third quadrant ($\omega < 0$ and $k < O$) gives right hand polarized MS waves propagating in the $+x$ direction, whereas, the fourth quadrant ($\omega < 0$ and $k > 0$) represents waves propagating in the negative x-direction. An MHD turbulence can be produced by superposition of waves with an arbitrary spectrum and polarization. Strong wave-particle interaction is produced when the cyclotron resonance condition (4) is satisfied.

Case ii) we consider particle interactions via cyclotron resonance with both elliptically and circularly polarized monochromatic *MS* waves propagating sunward obliquely to the background magnetic field.

Case iii) *MHD* "turbulence" generated by nonlinear *MS* waves propagating sunward and anti-sunward obliquely to the *IMF*:

The third type of calculation is made for turbulent magnetic fluctuations generated by elliptically/circularly polarized *MS* waves propagating in opposite directions obliquely to the average magnetic field via a cyclotron resonance. From Fig. 2, it can be seen that the ions moving along and opposite to x-direction have v >0 (v < O) and resonantly interact with R^+ waves (R^- waves). A turbulent wave-field is generated by superposing elliptically polarized magnetosonic waves propagating sunward and anti-sunward (+*x* and -*x* directions) obliquely to the background magnetic field. The components of wave magnetic field are given by

$$B_{wy} = \sum_{k_{min}}^{k_{max}} B_k^{yj} \cos(kx - \omega t + \phi_0) \tag{8}$$

$$B_{wz} = \sum_{k_{min}}^{k_{max}} B_k^{zj} \sin(kx - \omega t + \phi_0) \tag{9}$$

The coefficients are related to the power spectral density $P(k)$ as:

$$[\delta B_k]^2 = [B_k^{yj}]^2 + [B_k^{zj}]^2 = P(k)\ \Delta k \tag{lo}$$

where Ak is related to the length, *L*, of the simulation box as Ak = $2\pi / L$ and the power spectrum $P(k)$ is assumed to vary as k-y , and j refers to sunward and antisunward propagating waves . One writes $k = m\ Ak = m\ 2\pi /L$, where m is the mode number of

the waves in the system, The wave length, λ , of the mode m is given by L/m . For $B_k^{yj} = B_k^{zj}$ we get circularly polarized waves.

The amplitude of the turbulence is given by

$$[\delta B]^2 = \sum_{k_{min}}^{k_{max}} \{[B_k^{yj}]^2 + [B_k^{zj}]^2\} \tag{11}$$

Case iv) "Turbulent" MHD fluctuations generated by circularly polarized nonlinear MS waves propagating sunward:

The fourth type of calculation is made for turbulent magnetic fluctuations generated by elliptically/circularly polarized MS waves propagating obliquely to the IMF in one direction only (sunward), viz., along positive x-axis via a cyclotron resonance. A "turbulent" wave-field is generated by superposing circularly polarized magnetosonic waves. Eqs. (8)-(10) are valid in this case as well,

c) The Simulation System:

The simulation system is one dimensional in space, namely, x along the sun-comet line which is shown in Fig. 1. The direction of propagation of MS waves propagating sunward and anti-sunward coincides with the +x-axis and -x-axis. However, the ion trajectories, the velocities and the electromagnetic fields are three dimensional vectors. The background interplanetary magnetic field makes an angle θ_{Bk} with propagation vector. The resonant mode numbers of MS waves via a cyclotron resonance are calculated from

$$M_{res} = k_{res}/\Delta k = L\ k_{res} / 2\pi \tag{12}$$

where the system size, $L = NX\,c_A / \Omega_i$, ($ZW=512$ for the comet Halley and 128 for the comet G-Z is taken because the interacting region for the comet Halley is about four to eight times larger than that for the comet G-Z) is represented by 1024 grid points. Hence, we have

$$M_{res} = \frac{NX\ c_A}{2\pi\Omega_i} \frac{(\omega+\Omega_i)}{v_R \cos\theta_{Bk}} \qquad (13)$$

Here, V_R, c_A are, respectively, the resonance velocity and the Alfven velocity. The mode numbers are assumed to lie between 5 and 61.

The total electric field in the frame of reference moving with the plasma (the solar wind) is given by

$$(\delta \mathbf{E}) = -\bar{V_w} \times \bar{B_w} / c - \bar{V_w} \times \bar{B_0} / c \qquad (14)$$

where $\bar{V_w}$ is the wave velocity vector.

The three dimensional trajectories of the ions are obtained by numerically solving the equations of motion:

$$d\bar{r} / dt = V-, \qquad (15)$$

$$d\bar{v} / dt = \frac{e}{M_i} (\delta\bar{E} + \bar{v} \times \bar{B} / c) \qquad (16)$$

where $\bar{B} = \bar{B_o} + \bar{B}_w$, and $\bar{r} = \bar{i}\,x + \bar{j}\,y + \bar{k}\,z$, is the position vector, $\bar{v}$ is the velocity vector and M_i is the mass of cometary water group ion. The pitch angle scattering width, time averaged pitch angle frequency, average velocity, and root mean square deviation are calculated by using the test particle simulation code in the four cases.

Following Gary et al., [1991] and Srivastava et al., [1993] a time-averaged pitch-angle scattering *(TAPAS)* frequency ν_θ can be defined through the expression

$$< \Theta'(t) > = \frac{\pi - 2}{2} \exp(-\upsilon_\theta t) \tag{17}$$

where <0'> represents deviation from an isotropc distribution given by

$$< \Theta'(t) > = \frac{\pi - 2}{2} - < \Theta(t) > \tag{18}$$

and $< \Theta(t) >$ is the average width of pitch angle distribution.

Integrating Eq. (17) for large times, ν_θ can be approximated by

$$\nu_\theta / \Omega_i = (\pi/2 - 1) / \int_0^\infty \Theta' \ (t^*) \ dt^* \tag{19}$$

SIMULATION RESULTS

Test particle calculations are performed for resonant mode number range from 5 to 61 for various angles θ_{Bk}, α, and wave amplitudes. At $t^* = \Omega_i t$ = O, 1000 ions are injected uniformly into the simulation system with an injection velocity:

$$v_{0x} = v_{0b} \cos \phi \ , \ v_{0y} = v_{0b} \sin \phi \tag{20}$$

where $\phi = \alpha - \theta_{Bk}$

The amplitude of the nonlinear *MS* waves was varied from 0.5 to 0.8 for both the comets and that of the MS turbulence $(|\Delta B/B_0|)^2$ was varied from 0.12 to 0.25 for the comet Halley and from 0.4 to 0.5 for the comet *G-Z.* c_S/c_A for the comet Halley (*Coates* et al.,

1990) and for the comet G-Z (*Tsurutani*, 1991) are taken as 1.73 and 1.18 respectively. θ_{BK} is varied from 20" to 60" and α is varied from 45° to 85° in all the four cases. Pitch angle scattering rates as defined in Eq. (19), the average velocity and root mean square deviation are given in Tables 1-4 for comparison. Figures 3 through 10 show characteristic features of the study. In the cases of *i)* and *ii)*, the interaction regions (the length of the simulation system, $L = 128\, c_A/\Omega_i$) considered for the comets *Halley* and G-Z are assumed to have the same legth for the sake of comparison of results,

Case *i)* Monochromatic waves propagating sunward and anti-sunward obliquely to the *IMF*.

The results are given in Table 1*a* for the comet G-Z and in Table I*b* for the comet *Halley* for resonant mode number 6, α = 45° and θ_{Bk} = 20", 40", 50",60" and wave amplitudes 0.4, 0.4. It can be seen from Tables 1a and *2a* for the comet G-Z that time averaged pitch angle scattering rate *(TAPAS)* is higher for sunward-antisunward waves than that for sunward waves only due to certain stochasticity in the case of the former, The right hand part of Table la gives results for elliptically polarized waves for $A_{0z}/A_{0y} = 1.4$. Other parameters are the same as for *CPMSW*. It can be seen that PAS and acceleration in crease with the increase in the z-component of the wave magnetic field. In case $A_{0z}/A_{0y} < 1$, the *PAS* and acceleration are less than those in the case of *CPMSW*.

Figure *3* shows ($\Omega_i t, < v > /c_A$) relation for the comet G-Z for resonant mode number 16, α = 45", θ_{Bk} = 50° and *CPMS* wave of amplitudes 0.8,0.8. The three curves labelled I, II, 111 in Figure 3 refer respectively to the cases of sunward waves in the presence of uniform *IMF*, sunward waves with variable *IMF*, and sunward-antisunward waves with variable *IMF*. Naturally the pitch angle scattering and acceleration are larger due to stronger stochastic effects for sunward-antisunward propagating waves than those for

waves propagating sunward only which can be seen from the curves labelled II and 111. It can be seen from curves labelled I and II that oscillatory behaviour of average velocity reduces in the case of *IMF* with positive gradient (B_{0y} increasing towards the comet).

Case ii). Monochromatic waves propagating sunward obliquely to the *IMF*

The results are given in Table *2a* for the comet G-Z and in Table *2b* for the comet *Halley* for resonant mode number 6, $\alpha = 45°$ and θ_{Bk} = 20°, 40°, 50", 60° and wave amplitudes 0.5. It can be seen from Tables 1a and 2a for the comet G-Z and from Tables lb and 2b for comet *Halley* that *PAS* and average velocity are larger in the case of sunward-antisunward waves even with smaller amplitudes (0.4, 0.4) than those for sunward waves only with larger amplitude (0.5).

Figure 3 shows ($\Omega_i t$, $< v > /c_A$) relation for the comet G-Z for resonant mode number 16, a = 45", $\theta_{Bk} = 50°$ for *CPMS* waves of amplitudes 0.8. It can be seen from the curves labelled I and 11 that trapping of particles is reduced by the spatially dependent ambient magnetic field increasing towards the comet. The particles get more pitch angle scattered and more accelerated in the case of increasing magnetic field than that in the case of uniform *IMF*.

Water group ions get trapped in the case of monochromatic *MS* waves due to Landau damping. This is more obvious in the case of uniform *IMF* than that in the case of *IMF* with positive gradient. The mechanism for Landau damping of monochromatic *MS* waves has been discussed by Srivastava et al., (1993). The Landau damping rate of oblique nonlinear *MS* waves is given by Kotelnikov et al., (1991)

$$\gamma_L / \Omega_i = M (c_{ph}/c_A) \sin^2\theta_{Bk} \beta^{1/2} e^{-1/\beta} \qquad (21)$$

where M is the resonant mode number for the wave particle interaction which depends on the angle of injection, c_ph is the phase velocity of the *MS* waves and β is the solar wind plasma beta which varies from 0.01 to 0.1 in the solar corona, from 0.5 to 1 in the case of comet G-Z and from 1 to 3 in the case of comet *Halley*. Figure 4 shows Landau damping rate for different angles of propagation for different plasma conditions for comets.

Case iii) "Turbulent" magnetic fluctuations generated by nonlinear waves propagating sunward and anti-sunward obliquely to the *IMF*:

The results are given in Table *3a* for the comet G-Z and in Table *3b* for the comet *Halley* for a range of mode numbers 5-61, α = 45" and θ_{Bk} = 20", 40", 50°, 60" and wave amplitudes 0.5, 0.1 for the comet G-Z and 0.25, 0.05 for the comet Halley. As the antisunward waves are less turbulent and only 5 to 10 % of waves propagate in this direction , the amplitude of these waves is assumed to be 20 % of sunward propagating waves [Johnstone et al., 1992]. The waves at *Halley are* less turbulent and result in less *PAS* and acceleration than that in the case of comet G-Z. The right hand part of Table 3a shows results for *EPMSW* for B_k^{zj} / B_k^{yj} =1.2. The *PAS* and acceleration are larger for *EPMSW* than for *CPMSW*. In case $B_k^{zj} / B_k^{yj} < 1$, the *PAS* and acceleration are less than those for *CPMSW*.

The curves labelled II and III in Figure 5 show ($\Omega_i t, < v > /c_A$) relation for θ_{Bk}= 50°, α = 45°, and wave amplitudes equal to 0.4, 0.4 for the sunward-antisunward propagating waves for comet G-Z and 0.25, 0.25 for comet *Halley* and the curve 111 for the sunward propagating waves for the comet G-Z. Figure 6 shows (θ_{Bk}, σ_v/c_A) relation for different values of α for the same wave amplitudes for α = 45",65°, 85° for the comet

G-Z. Figure 7 shows time-averaged pitch angle scattering (*TAPAS*) rates for α = 45",65°, 85" for comet G-Z.

Case iv) "Turbulence" generated by circularly polarized nonlinear waves propagating sunward obliquely to the *IMF*:

The results are given in Table 4a for the comet G-Z and in Table *4b* for the comet *Halley* for a range of mode numbers 5-61, α = 45" and θ_{Bk} = 20", 40", 50°, 60" and wave amplitudes 0.4 for the comet *G-Z* and 0.25 for the comet *Halley*. Calculations have been performed for *CPMSW* as well as for *EPMSW* and it is found that the larger the z-component of the wave magnetic field, the larger is the *PAS* and acceleration of particles in agreement with the result for sunward-antisunward waves.

The curve labelled I in Figure 5 shows ($\Omega_i t$, < v > /c_A) relation for θ_{Bk} = 50°, α = 45", and wave amplitudes equal to 0.4 for sunward propagating waves. Figure 6 shows (θ_{Bk} , σ_v/c_A) relation for different values of α for the same wave amplitude. Figure 7 shows time-averaged pitch angle scattering *(TAPAS)* rates against θ_{Bk} for α = 45" for the comet *G-Z.*

v) Comparison of results for *EPMSW* and *CPMSW*:

We have obtained results for elliptically polarized waves for α = 45°, θ_{Bk} = 40" for monochromatic waves as well as for the turbulence generated by by *EPMSW* and compared with results foe *CPMS W*. For monochromatic *EPMS W* A_{0z} / A_{0y} is chosen as 1.4 and 0.8 and for turbulence generated by *EPMSW* B_k^{zj} / B_k^{yj} as 1.2 and 0.8. The results are shown in figures 8, 9 and 10. Figure 8 and 9 show results for sunward-antisunward and sunward propagating monochromatic *MS* waves respectively. Figure 10 shows results for a broad band spectrum of sunward-antisunward propagating *MS* waves.

It can be seen that *PAS* and average velocity of particles increase with the increase in the z-component of the wave magnetic field.

SUMMARY AND CONCLUSIONS

Tsurutani et al., (1987, 1989), noted that very far from the comet G-Z (7x105 km) waves were predominantly elliptically polarized, long wavelength *MHD* waves. At intermediate distances (≈ 3x105 km), the waves were more compressive. The steepened *MS* waves had partial (circularly polarized) rotation, linearly polarized portions and were sometimes preceded by high frequency wave packets. Near the comet (r < 2x105 km) the fluctuations had large amplitudes ($|\delta B/B_0| \approx 1$), were highly compression al, and had a "turbulent-like" power spectrum. It is thus obvious that different types of Alfvenic fluctuations are associated with different degrees of isotropization of the ion distributions. These observations suggest that it would be instructive to study the particle interactions with both the monochromatic waves and a broad band spectrum of waves with spectral index varying from -1.6 to -2.5. The present study of interaction of pickup ions with magnetosonic waves propagating both sunward and anti-sunward obliquely to the *IMF* via cyclotron resonance shows larger pitch angle scattering, and acceleration than those for the cases of parallel and anti-parallel propagating Alfven waves [*Terasawa*, 1989: *Cravens*, 1989: *Gary* et al., 1991] and unidirectionally sunward propagating waves [*Srivastava* et al., 1993]. This is mainly due to the following reasons: i) the amplitude of the *MS* waves is much larger than the parallel propagating Alfven waves, and ii) the component of the phase velocity of the waves (scattering center) parallel to the magnetic field for obliquely propagating *MS* waves is much larger than the Alfven velocity.

We have performed test particle calculations to study wave particle interactions via cyclotron resonance of water group cometary ions for four cases taking into account the decelerating solar wind flow due to mass loading: i) monochromatic waves propagating

both sunward and anti-sunward, ii) monochromatic waves propagating sunward unidirectionally, iii) a broad band spectrum, propagating both sunward and anti-sunward, and iv) a broad band spectrum, propagating sunward only. The power spectrum is assumed to vary as $1/k^2$ for both the waves propagating sunward and anti-sunward. The present study considers three new features of the wave-particle interaction in the cometary atmosphere as compared to the previous one (*Srivastava* et al., 1993). Firstly, it takes into account the observational input to the interplanetary magnetic field as given in Eq. (3), in agreement with the observations [Neugabauer et al., (1990)]. Secondly, it aims at a comparative study of wave particle interactions between sunward and anti-sunward propagating *MS* waves and sunward propagating waves only, for both the monochromatic waves and a broad band spectrum of waves. Thirdly calculations are made for *EPMSW* and compared with those of *CPMSW* which are shown in Figures 8, 9 and 10. This study is based on *MHD* dispersion relation for the *MS* waves whereas the previous one [*Srivastava* et al., 1993] used a kinetic dispersion relation. The difference between the results with the kinetic and *MHD* dispersion relation was found to be within 10%. In both the studies, it is found that efficient pitch angle scattering and acceleration of particles takes place. They are found to be much larger in the case of sunward-antisunward propagating waves than those for the sunward propagating waves only. This is because of the different stochastic effects associated with the two cases resulting in larger power for sunward-antisunward propagating waves than that for the sunward propagating waves only. The electromagnetic trapping of particles in the case of sunward-antisunward propagating waves is less than that in the case of sunward propagating waves only as can be seen from curves II and HI in Figure **3.** It is also noted that the trapping of particles by monochromatic *MS* waves is much reduced by a spatially dependent increasing *IMF*. The variable component of the *IMF*, namely, B_{0y} increases rapidly near the comet due to decelerating solar wind which causes more *PAS* and acceleration.

Pitch angle scattering and acceleration depend on θ_{Bk}, α, wave amplitudes and resonant mode numbers. *PAS* and acceleration increase with increasing wave amplitude. For monochromatic *MS* waves acceleration decreases with increasing resonant mode numbers because power associated with mode numbers decreases as mode numbers increase. It is found that acceleration increases with increasing θ_{Bk} in both the cases, namely, monochromatic waves and a broad band spectrum of waves due to larger phase velocity of waves increasing with the increase in θ_{Bk} and is larger for sunward-antisunward propagating waves than that for sunward propagating waves only due to stronger stochastic effects associated with the former. In the case of sunward-antisunward propagating waves *PAS* increases with the increase in θ_{Bk} upto 50" and then decreases whereas in the case of sunward propagating waves it decreases with the increase in θ_{Bk} upto 60° (θ_{Bk} >60" was not studied). It is due to its explicit dependence on θ_{Bk} and implicit dependence on α. For A >0,5 and L = 512 c_A/Ω_i, it increses with the increase in α and decreases with the increase in θ_{Bk}.

In both the cases, namely, monochromatic *MS* waves and *MHD* "turbulence" generated by a broad band spectrum of *MS* waves, the average velocity of particles depends on the value of plasma beta. In the cases of *MHD* "turbulence" (cases iii and iv) the maximum of <v> occurs at θ_{Bk} -70"-75" for c_S/c_A = 1.73 and at θ_{Bk} =50°-55° for c_S/c_A = 2.36.
For θ_{Bk} =20", *PAS* and acceleration increase as α increases. For θ_{Bk} lying between 30° and 60" *PAS* decreases as α increases but average velocity increases as α increases. This is due to the explicit dependence of $\nu_{|||}$ on θ_{Bk} and its implicit dependence on α. In the case of comet Halley, *TAPAS* rate increases with the increase in both θ_{Bk} and α. In the case of comet G-Z *PAS* decreases with the increase in θ_{Bk}. *TAPAS* rate for G-Z increases with the increase in α for θ_{Bk} >40°. This is probably because the waves at Halley have lower amplitude and are more turbulent than those at comet G-Z where they are less turbulent but have larger amplitudes.

It is found that pitch angle scattering, average velocity and acceleration increase with the increase in the ratio A_{0z}/A_{0y} in the case of monochromatic elliptically polarized MS waves and with the increase in B_k^{zj}/B_k^{yj} in the case of broad band spectrum of elliptically polarized MS waves . This implies that increase in the z-component or decrease in the y-component of the wave magnetic field causes increase in the pitch angle scattering and acceleration.

Acknowledgements:

This work was done at the Jet Propulsion Laboratory, California Institute of Technology under contract with the National Aeronautics and Space Administration. Also, this work was performed during the period Krishna M. Srivastava held a Senior Resident Research Associateship administered by the National Aeronautics and Space administration through the National Research Council. Useful discussions with M. Neugebauer, B. Goldstein and R. Goldstein are thankfully acknowledged.

REFERENCES:

Coates A. J., B. Wilken, A, D. Johnstone, K. Jockers, K.-H. Glassmeier, and D. E. Huddleston, Bulk properties and velocity distributions of water group ions at comet Halley: Giotto measurements, *J. Geophys. Res.*, 95, 10249, 1990.

Coates, A. J., A. D. Johnstone, D. E. Huddleston, B. Wilken, K. Jockers, and K. -H. Glassmeier, Velocity space diffusion of pickup ions from the water group at comet Halley, *J. Geophys. Res.*, 94, 9983, 1989; *Correction, J. Geophys. Res., 95, 4343,1990.*

Cravens, T. E., Test particle calculations of pickup ions in the vicinity of comet Giacobini-Zinner, *Planet. Space Sci, 37,* 1169, 1989.

Gary, S. P., R. H. Miller and D. Winske, Pitch angle scattering of cometary ions: Computer simulation, *Geophys. Res. Lett., 18,* 1067, 1991.

Huddleston, D. E., A. D. Johnstone, and A. J. Coates, Determination of comet Halley gas emission characteristics from mass loading of the solar wind, *J. Geophys. Res.*, 95, 21, 1990.

Johnstone, A, D., D. E. Huddleston, and A. J. Coates, Analysis of the spectrum of cometary pickup waves using Elsasser variables, Cospar Colloquim, University of Michigan, Ann Arbor, 1992.

Kotelnikov, A. D., M. A, Polyudov, M. A. Malkov, R. Z. Sagdeev, and V. D. Shapiro, High amplitude magnetosonic waves in the upstream region of the cometary bow shock, *Astron. Astrophys., 243,546,1991.*

Neubauer, F. M., and 11 coauthors, First results from the Giotto magnetometer experiment at comet Halley, *Nature, 321,* 352, 1986.

Neugebauer, M., A. J. Lazarus, H. Balsiger, S. A. Fuselier, F. M. Neubauer, and H. Rosenbauer, The velocity distribution of cometary protons picked up by the solar wind, *J. Geophys. Res.*, 94, 5227, 1989.

Neugebauer, M., A. J. Coates, and F. M. Neubauer, Comparison of picked up protons and water group ions upstream of comet Halley's bow shock, *J. Geophys. Res.*, **95, 18745, 1990.**

Srivastava, K. M., B. T. Tsurutani, and B. E. Goldstein, Pitch angle scattering of cometary ions due to MHD turbulence generated by obliquely propagating nonlinear magnetosonic waves, *COSPAR Colloquim, University of Michigan,1992, (in Press).*

Srivastava, K. M., B. T. Tsurutani, and B. E. Goldstein, Acceleration of cometary H20 group pickup ions by obliquely propagating nonlinear magnetosonic waves (and references therein), *J. Geophys. Res.* , 1993, (in Press).

Terasawa, T., Particle scattering and acceleration in a turbulent plasma around comets, *Geophysical Monograph, 53,41, 1989.*

Thorne, R. M. and B. T. Tsurutani, Resonant interactions between cometary ions and low frequency electromagnetic waves, *Planet. Space Sci., 35, 1501, 1987,*

Tsurutani, B. T., R. M, Thorne, E. J. Smith, J. T, Gosling, and H. Matsumoto, , Steepened magnetosonic waves at comet Giacobini Zinner, J. Geophys. Res., 92, 11074, 1987.

Tsurutani, B. T., Cometary plasma waves and instabilities in *Comets in the Post-Halley Era, 2,* 1171, 1991 a.

Tsurutani, B, T., Nonlinear low frequency (LF) waves: Comets and Foreshock Phenomena, in Physics of Space Plasmas, edited by T. Chang, G. B. Crew and J. R. Jasperse (1991 b).

Tsurutani, B. T., D. J. Southwood, E. J. Smith and A. Balogh, Nonlinear magnetosonic waves and mirror mode structures in the March 1991 Ulysses interplanetary event, Geophys. Res. Lett., 1,9,1267,1992.

Ye, G., and T. E. Cravens, Combined energy and pitch angle diffusion of pickup ions at comet Halley, *J. Geophys. Res. Lett.*, 96,5479, 1991.

Ye, G., T. E. Cravens, and T. I. Gombosi, Pickup protons and water ions at comet Halley: Comparisons with Giotto observations, *J. Geophys. Res.* ,98, 1311, 1993.

Figure Captions:

Fig. 1. Schematic diagram of the simulation geometry.

Fig, 2. MS wave dispersion relation and cyclotron resonance condition at points R^+ and R^- for ions moving in the +x and -x directions.

Fig. 3. $(\Omega_i t, \langle v \rangle / c_A)$ relation for monochromatic sunward-antisunward propagating waves for resonant mode number 16, α = 45" and θ_{Bk} = 50" and wave amplitudes 0,8, 0.8. Curve II refers to monochromatic sunward propagating waves of the same amplitude with variable IMF. Curve III refers to monochromatic upstream propagating waves with uniform IMF.

Fig. 4. (θ_{Bk}, γ_L) relation for MS waves of mode number 26, β = 0.5, 1.0, 1.5 for α =55° obtained from Eq. (25) for the comet G-Z and Halley.

Fig. 5. $(\sigma_v/c_A, \langle v \rangle / c_A)$ relation for "turbulent" sunward-antisunward propagating waves for Halley and G-Z and "turbulent" sunward propagating waves for resonant mode number range 5-61 , α = 45° and θ_{Bk} = 50" and wave amplitudes 0.4, 0.4 for comet G-Z and 0.12, 0.12 for Halley.

Fig. 6. $(\theta_{Bk}, \sigma_v/c_A)$ relation for "turbulent" sunward-antisunward propagating waves for G-Z for resonant mode number range 5-61, α = 45°,65°, 85" and wave amplitudes 0.4, 0.4 for comet G-Z. The bottom curve corresponds to sunward propagating waves.

Fig. 7. $(\theta_{Bk}, \nu_\theta/\Omega_i)$ relation for "turbulent" sunward-antisunward propagating waves G-Z and "turbulent" sunward propagating waves for resonant mode number range 5-61, α = 45" , 65° , 85° and wave amplitudes 0.4, 0,4 for comet G-Z . The bottom curve corresponds to sunward propagating waves.

Fig. 8. $(\Omega_i t, \langle v \rangle / c_A)$ relation for monochromatic waves propagating both sunward and antisunward. Curve labelled I refers to circularly polarized waves and curves II and HI refer to elliptically polarized waves for A_{0z} / A_{0y} = 1.4 and 0.8.

Fig. 9. ($\Omega_i t, \langle v \rangle / c_A$) relation for monochromatic waves propagating sunward only. Curve labelled I refers to a broad band spectrum of circularly polarized waves and curves II and III refer to a broad band spectrum of elliptically polarized waves for A_{0z} / A_{0y} = 1.4 and 0.8.

Fig. 10. ($\Omega_i t, \langle v \rangle / c_A$) relation for the case of turbulence generated by a broad band spectrum of monochromatic waves propagating sunward-antisunward. Curve labelled I refers to a broad band spectrum of circularly polarized waves and curves II and III refer to a broad band spectrum of elliptically polarized waves for B_k^{zj} / B_k^{yj} = 1.2 and 0.8.

Table la. Sunward-Antisunward Propagating Monochromatic MS waves (G-Z),

	CPMSW				EPMSW , A_{0z}/A_{0y} = 1.4			
	M= 6				M= 6			
θ_{Bk} =	20°	40”	50°	60”	20”	40°	500	60°
ν_s/Ω_i =	**2.29**	**2.95**	**3.04**	**2,38**	**2.45**	**2.60**	**2.76**	**2.50**
σ_v /c_A	1.82	**3.63**	**3.89**	**3.99**	**3.73**	**4.05**	**4.29**	**4.35**
<v> /c_A	5.73	9.12	10.58	10.8	8.52	10.73	12.08	11.34

All values are at?* =200, α = 45”, L=128c_A/Ω_i , Δx=0.125, At =0.0125, A=O.4, 0.4, c_s/c_A =1.18, v_{0b} = 5 c_A.

Table lb. Sunward-Antisunward Propagating Monochromatic MS waves (Halley).

ν_s/Ω_i =	1.97	2.43	2.50	1.99
σ_v /c_A	**1.62**	**4.11**	**4.25**	**4.11**
<v> /c_A	**5.61**	**9.41**	10.2	9.41

All values are at t* =200, α = 45’, L=128c_A/Ω_i , Δx=0. 125, At =0.0125, A=0.25, 0.25, c_s/c_A = 1.73, v_{0b} = 5 c_A..

Table 2*a*. Sunward Propagating Waves Only (G-Z).

θ_{Bk} =	20”	40°	50”	60”
ν_ϑ/Ω_i =	1.77	2.22	2.32	2.46
σ_v/c_A	0.63	2.32	2.92	3.69
$\langle v \rangle/c_A$	**5.37**	**7.10**	**8.44**	**9.98**

All values are at $t^* = 100$, $\alpha = 45$”, A=O.5, $c_s/c_A = 1.18$, $v_{0b} = 5\ c_A$.

Table 2*b*. Sunward Propagating Waves Only (Halley) .

ν_ϑ/Ω_i =	**0.78**	**2.12**	**2.21**	**2.48**
σ_v/c_A	**0.26**	**2.05**	**2.78**	**3.21**
$\langle V \rangle/c_A$	5.62	6.63	7.89	8.96

All values are at f* =100, $\alpha = 45°$, $A = 0.3$, $c_s/c_A = 1.73$, $v_{0b} = 5\ C_A$.

Table 3a. Sunward-Antisunward Propagating Waves, (G-Z) MHD "Turbulence"

α	M= 5-61 A=O.5, 0.1 CPMSW			M= 5-61 A=O.5, 0.1 EPMSW , B_k^{zj}/B_k^{yj} = 1.2			
45° θ_{Bk} =	20°	400	50°	600	200	40"	500	60"
ν_θ/Ω_i =	1.75	1.53	1.57	1.71	1.73	1.60	1.58	1.61
σ_v/c_A	2.82	3.30	3.72	3.84	3.30	3.92	4.72	4.73
$\langle v \rangle/c_A$	7.37	8.86	10.4	9.68	8.20	10.53	11.58	11.54

All values are at t* =200, c_S/c_A =1.18, v_{0b} = 5 c_A , L=128c_A/Ω_1 , Δx=0. 125, Δt= 0.025 .

Table 3*b*. Sunward-Antisunward Propagating Paves (Halley).

45° θ_{Bk} =	20°	40"	50°	60"
ν_θ/Ω_i =	0.57	0.76	0.73	0.74
σ_v/c_A	1.87	2.84	3.94	6.02
$\langle v \rangle/c_A$	6.04	8.50	10.45	10.94

All values are at t* =200, c_S/c_A = 1.73, v_{0b} = 5c_A ,L=512 c_A/Ω_i, Δx=0.5, At=O.05, A=O.25, 0.05.

Table *4a.* Sunward Propagating Waves Only (G-Z)

45" θ_{Bk} =	20"	40"	50°	60°
ν_θ/Ω_i =	1.31	1.26	1.02	0.84
σ_v/c_A	**3.95**	**3.55**	**3.56**	**3.81**
$\langle v \rangle/c_A$	9.48	8.77	8.43	8.64

All values are at t^* =200, α = 45°, A=0.4, c_S/c_A=1.18, L=128 c_A/Ω_i , Δx=0.125, Δt=0.025.

Table *4b.* Sunward Propagating Waves Only, Comet Halley

ν_θ/Ω_i =	0.57	0.50	0.42	0.33
σ_v/c_A	2.63	2.65	2.86	3.03
$\langle v \rangle/c_A$	**6.83**	**7.08**	**7.91**	**8.54**

All values are at t^* =200, α = 45", A=O.25, c_S/c_A = 1,73, L=512c_A/Ω_i , Δx=0.5, At=O.05.

c_{ph}/c_A for the comet Halley (c_S/c_A = 1.732)

1.78 1.87 1.91 1.95

c_{ph}/c_A for the comet Giacobini-Zinner (c_S/c_A = 1. 18)

1.285 1.41 1.46 1.498

c_{ph} is the phase velocity of MS waves, c_S , and CA are the sound and Alfven speeds.

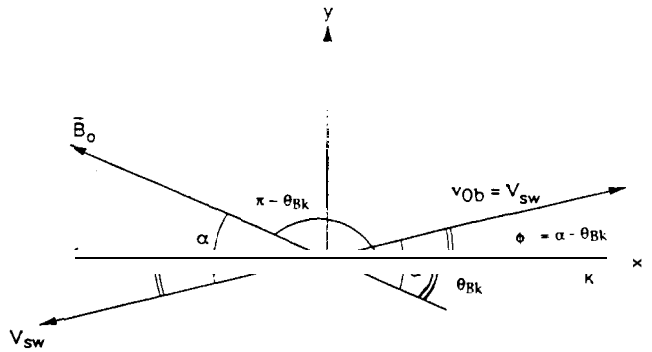

$v_{inj,x} = v_{0b} \cos\phi \quad v_{inj,y} = v_{0b} \cdot \sin\phi$

$\phi = \alpha - \theta_{Bk}$

$v_{\parallel B} = -v_x \cos\theta_{Bk} + v_y \sin\theta_{Bk}$

$v_{\perp B} = [(v_x \sin\theta_{Bk} + v_y \cos\theta_{Bk})^2 + (v_z)^2]^{1/2}$

Fig. 1

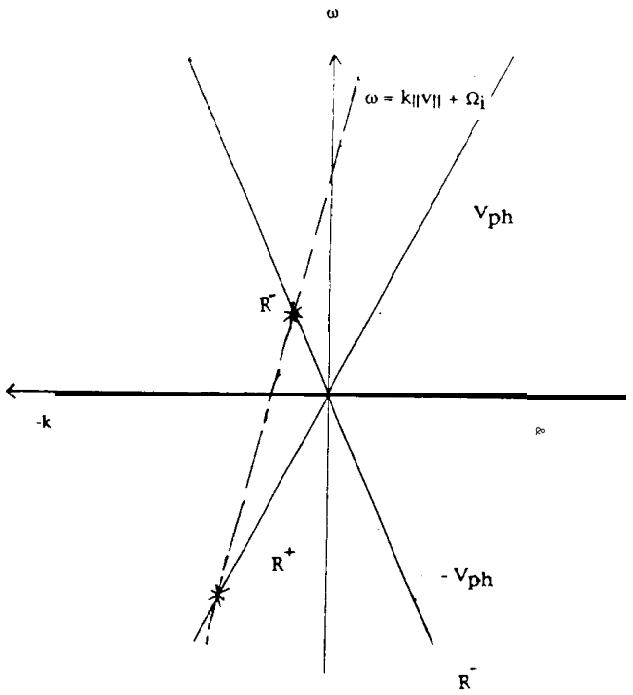

Fig. 2

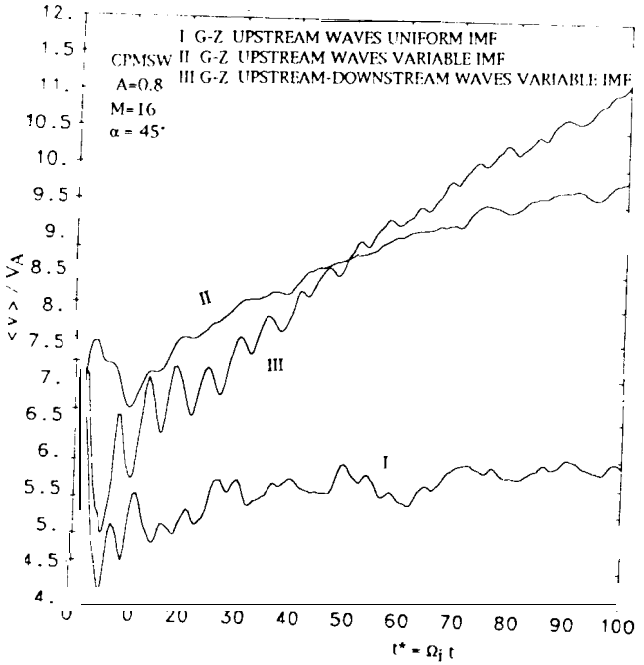
I G-Z UPSTREAM WAVES UNIFORM IMF
II G-Z UPSTREAM WAVES VARIABLE IMF
III G-Z UPSTREAM-DOWNSTREAM WAVES VARIABLE IMF
CPMSW
A=0.8
M=16
α = 45°
< v > / VA
t* = Ωi t
I
II
III

Fig. 3

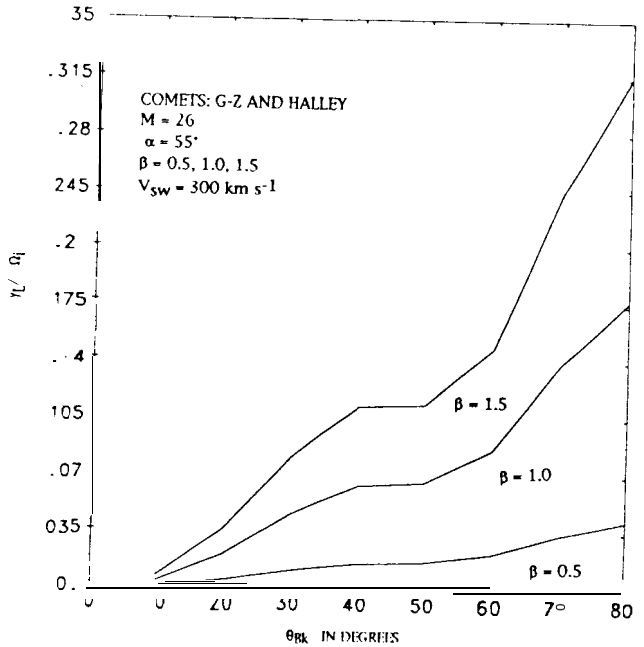
35
.315
.28
245
.2
175
.4
105
.07
035
0.
COMETS: G-Z AND HALLEY
M = 26
α = 55°
β = 0.5, 1.0, 1.5
V_{sw} = 300 km s^{-1}
γ_L / Ω_i
β = 1.5
β = 1.0
β = 0.5
0
20
30
40
50
60
70
80
θ_{Bk} IN DEGREES

Fig. 4

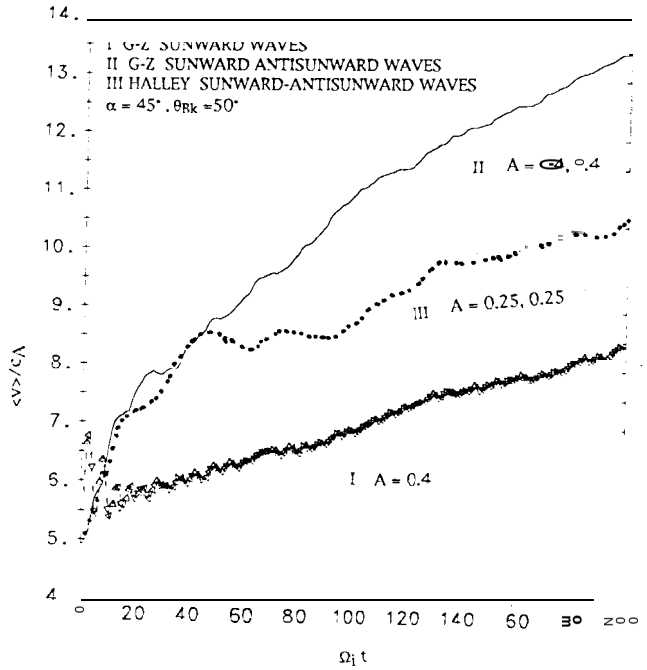
I G-Z SUNWARD WAVES
II G-Z SUNWARD ANTISUNWARD WAVES
III HALLEY SUNWARD-ANTISUNWARD WAVES
α = 45°, θBk =50°
II A = 0.4
III A = 0.25, 0.25
I A = 0.4
<v>/cA
Ωi t

Fig. 5

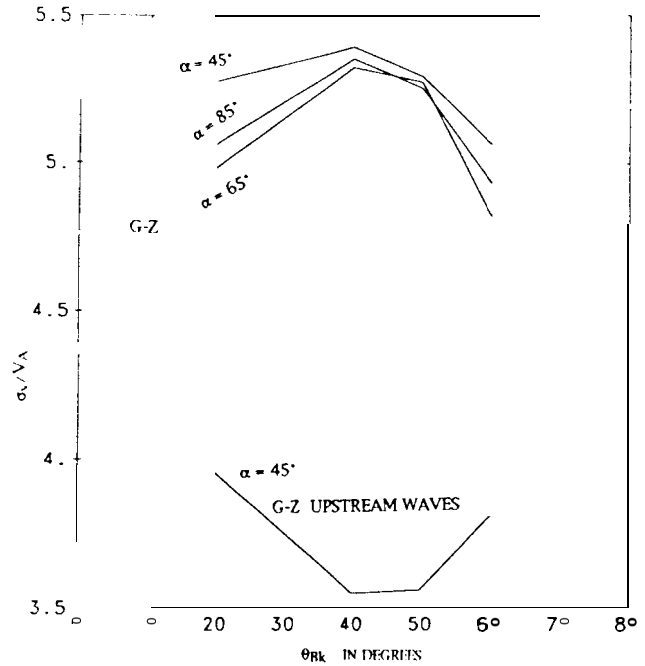
5.5
5.
4.5
4.
3.5
0
σ_r/V_A
α = 45°
α = 85°
α = 65°
G-Z
α = 45°
G-Z UPSTREAM WAVES
0
20
30
40
50
60
70
80
θ_{Bk} IN DEGREES

Fig. 6

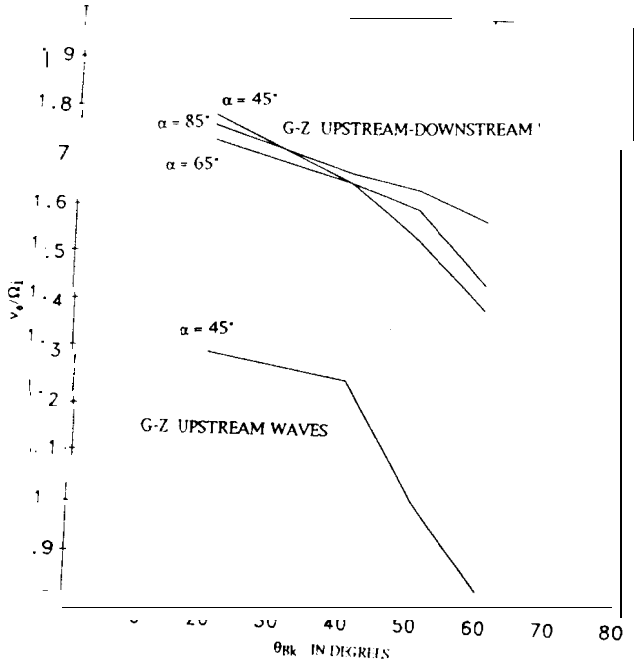
α = 45°
α = 85°
G-Z UPSTREAM-DOWNSTREAM
α = 65°
α = 45°
G-Z UPSTREAM WAVES
1.9
1.8
1.6
1.5
1.4
1.3
1.2
1.1
1
.9
50
60
70
80
θBk IN DEGREES

Fig. 7

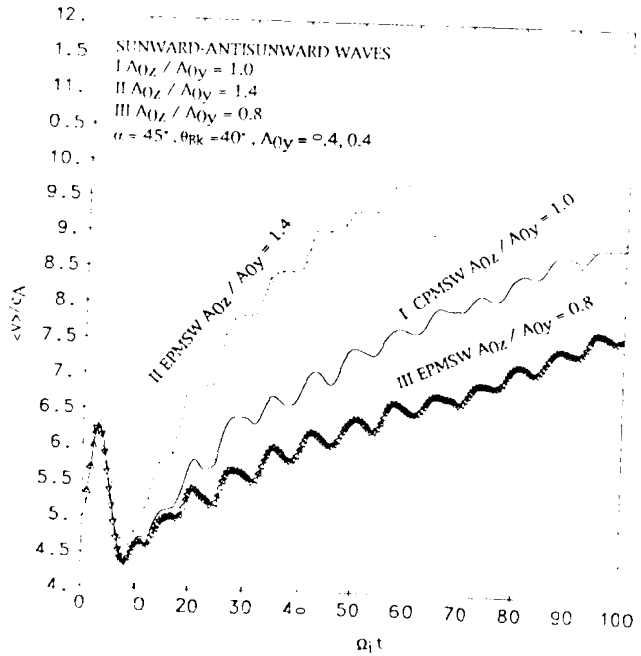
SUNWARD-ANTISUNWARD WAVES
I A0z / A0y = 1.0
II A0z / A0y = 1.4
III A0z / A0y = 0.8
α = 45°, θBk = 40°, A0y = 0.4, 0.4
II EPMSW A0z / A0y = 1.4
I CPMSW A0z / A0y = 1.0
III EPMSW A0z / A0y = 0.8
<v>/cA
ωi t

Fig. 8

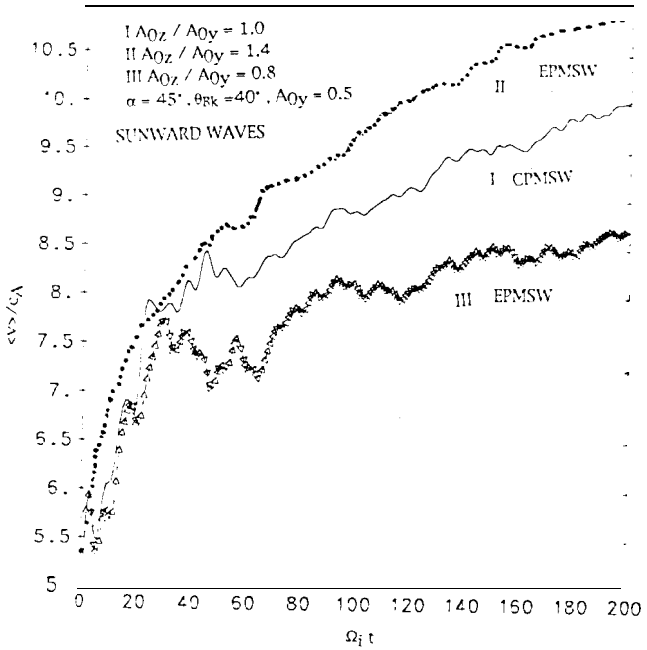
I A_{0z} / A_{0y} = 1.0
II A_{0z} / A_{0y} = 1.4
III A_{0z} / A_{0y} = 0.8
α = 45°, θ_{Bk} =40°, A_{0y} = 0.5
SUNWARD WAVES
II EPMSW
I CPMSW
III EPMSW
V_{ph}/V_A
Ω_i t
10.5
10.
9.5
9.
8.5
8.
7.5
7.
6.5
6.
5.5
5
0
20
40
60
80
100
120
140
160
180
200

Fig. 9

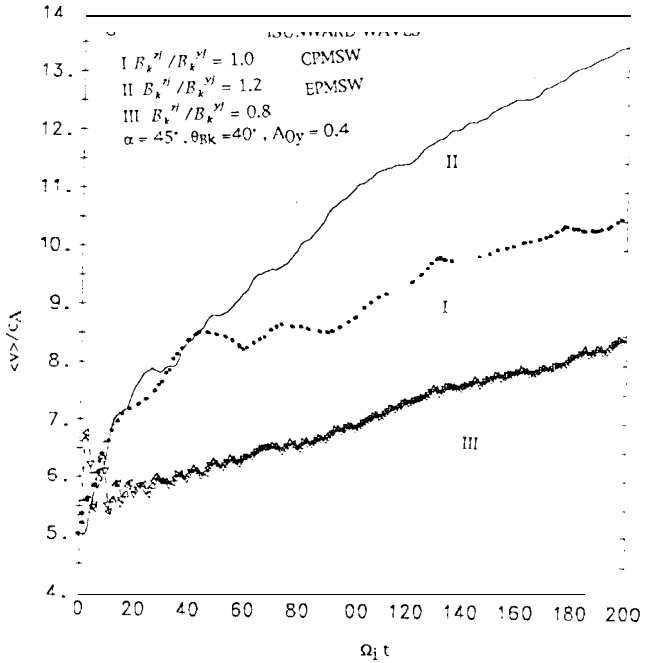
I B_k^{zj}/B_k^{yj} = 1.0 CPMSW
II B_k^{zj}/B_k^{yj} = 1.2 EPMSW
III B_k^{zj}/B_k^{yj} = 0.8
α = 45°, θBk =40°, A0y = 0.4
II
I
III
<v>/cA
Ωi t
14
13
12
11
10
9
8
7
6
5
4
0
20
40
60
80
00
120
140
160
180
200

Fig. 10